

Electrophilic Methylplatinum Complexes: A Theoretical Study of the Mechanism of C–C and C–H Bond Formation and Activation

Geoffrey S. Hill and Richard J. Puddephatt*

Department of Chemistry, University of Western Ontario, London, Canada N6A 5B7

Received October 23, 1997

The reductive elimination of methane or ethane from the five-coordinate intermediate model complexes $[\text{PtHMe}_2\text{L}_2]^+$, or $[\text{PtMe}_3\text{L}_2]^+$ respectively, and the corresponding C–H or C–C bond activation from the alkane complexes $[\text{PtMe}(\text{CH}_4)\text{L}_2]^+$ or $[\text{PtMe}(\text{C}_2\text{H}_6)\text{L}_2]^+$, respectively, have been studied by carrying out extended Huckel molecular orbital (EHMO) calculations and density functional theory (DFT) calculations on both the ground-state and transition-state structures with $\text{L} = \text{NH}_3$ or PH_3 . The EHMO calculations on *trans*- $[\text{PtL}_2\text{Me}_3]^+$, $\text{L} = \text{PH}_3$, show that the regular trigonal-bipyramidal (TBP) structure has an orbitally degenerate ground state and should undergo distortion to either the square-pyramidal (SP) or pinched trigonal-bipyramidal (PTBP) structure. In the PTBP structure, two methyl groups are in close proximity (C–Pt–C ca. 70°) and tilted away from each other. Although the tilting leads to a close Pt \cdots HC contact, no attractive agostic Pt \cdots H bonding is indicated. The DFT calculations predict that C–H reductive elimination and oxidative addition are much easier than C–C reductive elimination and oxidative addition, but there is no major difference between the activation energies when $\text{L} = \text{NH}_3$ or PH_3 . However, the platinum(IV) complexes are relatively more stable when $\text{L} = \text{NH}_3$ than when $\text{L} = \text{PH}_3$ compared to the platinum(II) alkane complexes, and so the activation energies for C–H or C–C oxidative addition are calculated to be lower for the NH_3 complexes. The platinum(IV) complexes with ligands L mutually cis or trans are most stable in the SP or PTBP stereochemistry, respectively. In the platinum(II) alkane complexes, the stereochemistry with ligands L mutually trans is preferred. The oxidative-addition/reductive-elimination reactions occur by a concerted mechanism, probably with a PTBP complex on the reaction coordinate. For C–H reductive elimination, the methane remains coordinated to platinum through the C–H σ complex. For C–C reductive elimination, the transition state is a C–C σ complex but in the final ethane complex the binding is as a C–H σ complex. For methane complexes, the binding is η^3 but one platinum C–H contact is shorter than the other, while for ethane complexes, the binding is usually η^4 through two eclipsed platinum C–H σ -complex interactions, but one appears much stronger than the other. The weaker of these σ -complex interactions is just strong enough to overcome the tendency of ethane to adopt the staggered conformation (ca. 3 kcal mol $^{-1}$). Activation of the C–C bond of ethane is likely only in systems where the much easier C–H activation is rapid and reversible.

Introduction

The activation of saturated hydrocarbons by oxidative addition of either C–H or C–C bonds to transition-metal complexes is an area of chemistry where there have been major advances but where many challenges remain.^{1–4} Because of the inherent difficulties in studying C–C and C–H bond oxidative additions directly,

much of the insight into alkane activation reactions has come from studying the microscopic reverse reactions, namely C–C and C–H bond reductive eliminations.¹ Since platinum(II) complexes are active in alkane activation and methylplatinum(IV) complexes are well-suited to studies of reductive elimination, there has been both experimental and also theoretical interest in both C–C and C–H bond-forming reactions.^{2,4–8} In addition, there is evidence for C–H bond activation by platinum(II),^{1,2,5} although C–C bond activation is easy only with strained hydrocarbons such as cyclopropane.⁹

Complexes of the type $[\text{PtMe}_2(\text{R})\text{XL}_2]$ ($\text{R} = \text{Me}, \text{H}; \text{X}$

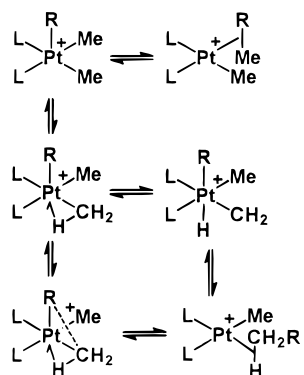
(1) (a) Shilov, A. E. *Activation of Saturated Hydrocarbons by Transition Metal Complexes*; Riedel: Dordrecht, The Netherlands, 1984. (b) Collman, J. P.; Hegedus, L. S.; Norton, J. R.; Finke, R. G. *Principles and Applications of Organotransition Metal Chemistry*; University Science Books: Mill Valley, CA, 1987. (c) Arndtsen, B. A.; Bergman, R. G.; Mobley, T. A.; Peterson, T. H. *Acc. Chem. Res.* **1995**, *28*, 154.

(2) (a) Holtcamp, M. W.; Labinger, J. A.; Bercaw, J. E. *J. Am. Chem. Soc.* **1997**, *119*, 848. (b) Stahl, S. S.; Labinger, J. A.; Bercaw, J. E. *J. Am. Chem. Soc.* **1996**, *118*, 5961.

(3) (a) Hutson, A. C.; Lin, M.; Basickes, N.; Sen, A. *J. Organomet. Chem.* **1995**, *504*, 69.

(4) (a) Low, J. J.; Goddard, W. A. *J. Am. Chem. Soc.* **1986**, *108*, 6115. (b) Low, J. J.; Goddard, W. A. *Organometallics* **1986**, *5*, 609.

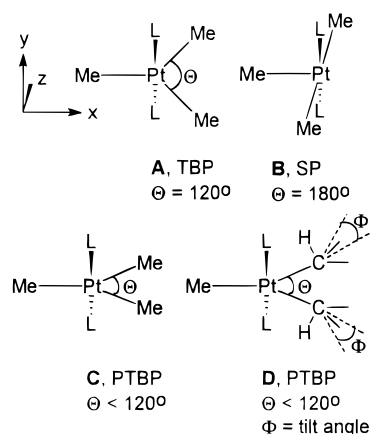
(5) (a) Hill, G. S.; Vittal, J. J.; Puddephatt, R. J. *Organometallics* **1997**, *16*, 1209. (b) Hill, G. S.; Puddephatt, R. J. *J. Am. Chem. Soc.* **1996**, *118*, 8745. (c) Hill, G. S.; Rendina, L. M.; Puddephatt, R. J. *Organometallics* **1995**, *14*, 4966. (d) Jenkins, H. A.; Yap, G. P. A.; Puddephatt, R. J. *Organometallics* **1997**, *16*, 1946.

Scheme 1^a^a R = H or Me.

= Me, halide; L = neutral ligand or L₂ = chelating ligand) are convenient substrates for studying the mechanisms of C–C and C–H bond reductive-elimination reactions from platinum(IV), and the following general conclusions have been drawn. Reductive elimination occurs from a five-coordinate intermediate which is formed by preliminary ligand dissociation.^{2,5–8} For the complexes [PtMe₃XL₂], X = halide or methyl, a ligand L normally dissociates and the intermediate is [PtMe₃XL] (L = tertiary phosphine or isocyanide ligand). If L₂ is a bidentate ligand which does not easily dissociate, then loss of X[–] occurs instead when X = halide and the five-coordinate intermediate is [PtMe₃L₂]⁺. The complexes *fac*-[Pt(H)Me₃(LL)] and [PtMe₄(LL)], which have no ligand that can easily dissociate, are stable to reductive elimination.^{5,6,10} On the other hand, complexes such as [PtHMe₂(O₃SCF₃)(bipy)], bipy = 2,2'-bipyridine, or [PtMe₃(O₃SCF₃)(dppe)], dppe = Ph₂PCH₂-CH₂PPh₂, which contain the very labile triflate ligand, undergo very easy C–H or C–C reductive elimination, respectively, since the five-coordinate intermediate is very easily accessible.⁵ If either C–H or C–C reductive elimination is possible, for example from the intermediates [PtHMe₂L₂]⁺, C–H reductive elimination is always observed.^{2,4–6} Reductive elimination from [PtMe₃XL₂] occurs more easily if L₂ is a diphosphine ligand such as dppe than if it is a diimine ligand such as bipy.^{7,11}

These are the experimental observations. The mechanism of C–H reductive elimination is thought to be concerted, giving a methane C–H σ-complex intermediate.^{1,2,4–6} The mechanism of C–C reductive elimination is less clear. Initially, a similar ethane C–C σ complex was proposed (Scheme 1, top), but then it was

Chart 1

^a L = PH₃.

suggested that preliminary tilting of one or both methyl groups should occur to enable C–C bond formation and that this would naturally lead to an agostic PtCH unit, leading to an ethane C–H σ complex instead (Scheme 1).^{7,8} The intermediacy of carbene complexes following an agostic intermediate and then α-elimination (Scheme 1) has not been completely eliminated. The problem in obtaining a definitive answer to this mechanistic question arises from the inability to detect any of these proposed five-coordinate or σ-complex intermediates or transition states by spectroscopic methods, so that only indirect evidence, especially from isotope effects, is available.^{2,8}

Because of the difficulties involved in the direct study of these proposed σ complexes, it was decided to follow a theoretical approach, and this paper reports the results obtained. A preliminary qualitative study using EHMO theory is given and then geometrical optimizations of the starting materials, products, and transition states are given for MeR reductive elimination/oxidative addition between complexes of the type [PtMe₂(R)L₂]⁺ and [PtMe(MeR)L₂]⁺ (R = Me, H; L = NH₃, PH₃) using density functional theoretical (DFT) calculations. Theoretical studies of reductive elimination from platinum(IV) have been made before⁴ but not on the five-coordinate intermediates and not using DFT. It has been established previously that the concerted reductive-elimination reactions are orbitally allowed.^{8,12}

Results and Discussion

Preliminary Considerations and EHMO Calculations.¹² Most five-coordinate complexes have trigonal-bipyramidal (TBP) or square-pyramidal (SP) stereochemistry, but the TBP structure is not favored for a metal complex having a d⁶ electron configuration. This is shown for the present case by carrying out EHMO calculations on the model complex cation [PtMe₃(PH₃)₂]⁺, A, Chart 1, for simplicity choosing the structure with a linear PtP₂ group. This will not necessarily be the most stable geometry (at least in the square-pyramidal form where there will be two mutually trans methyl groups), but this is not a primary consideration at this point. Figure 1 shows an energy correlation

(12) Komiya, S.; Albright, T. A.; Hoffmann, R.; Kochi, J. K. *J. Am. Chem. Soc.* **1976**, *98*, 7255.

(6) (a) O'Reilly, S. A.; White, P. S.; Templeton, J. L. *J. Am. Chem. Soc.* **1996**, *118*, 8, 5684. (b) Canty, A. J.; Dedieu, A.; Jin, H.; Milet, A.; Richmond, M. K. *Organometallics* **1996**, *15*, 2845. (c) De Felice, V.; De Renzi, A.; Panunzi, A.; Tesauro, D. *J. Organomet. Chem.* **1995**, *488*, C13.

(7) (a) Goldberg, K. I.; Yan, J.; Breitung, E. M. *J. Am. Chem. Soc.* **1995**, *117*, 6889. (b) Goldberg, K. I.; Yan, J.; Winter, E. L. *J. Am. Chem. Soc.* **1994**, *116*, 1573.

(8) (a) Brown, M. P.; Puddephatt, R. J.; Upton, C. E. E. *J. Chem. Soc., Dalton Trans.* **1974**, 2457. (b) Brown, M. P.; Puddephatt, R. J.; Upton, C. E. E. *J. Organomet. Chem.* **1973**, *49*, C61. (c) Roy, S.; Puddephatt, R. J.; Scott, J. D. *J. Chem. Soc., Dalton Trans.* **1989**, 2121.

(9) Jennings, P. W.; Johnson, L. L. *Chem. Rev.* **1994**, *94*, 2241.

(10) (a) Lashanizadehgan, M.; Rashidi, M.; Hux, J. E.; Puddephatt, R. J.; Ling, S. S. M. *J. Organomet. Chem.* **1984**, *269*, 317. (b) Goldberg, K. I. personal communication. (c) Hill, G. S.; Puddephatt, R. J. *Organometallics* **1997**, *16*, 4522.

(11) Crespo, M.; Puddephatt, R. J. *Organometallics* **1987**, *6*, 2548. Thermolysis of [PtXMe₃(bipy)] gives mostly methane rather than ethane.

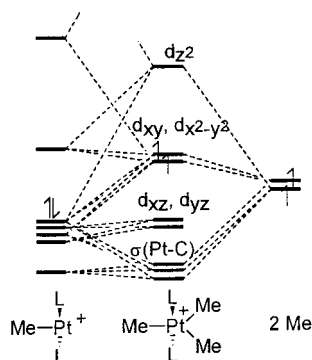


Figure 1. Energy correlation diagram for the formation of trigonal-bipyramidal $[\text{PtMe}_3\text{L}_2]^+$, A, L = PH_3 , from $[\text{PtMeL}_2]^+$ and two methyl radicals. A paramagnetic ground state is predicted, and Jahn–Teller distortion is expected to occur.

diagram for the formation of the trigonal-bipyramidal complex from T-shaped $[\text{MePt}(\text{PH}_3)_2]^+$ (the expected product of the reductive elimination) and angular ($2 \times \text{Me}$) fragments.

If we take the PtP_2 axis as z , the frontier orbitals are hybrids¹² that have mostly platinum 5d-character with the d_z^2 orbital at the highest energy and then the essentially degenerate d_{xy} , $d_{x^2-y^2}$ orbitals and then the d_{xz} , d_{yz} orbitals. For a d^6 complex, the first four electrons fill the d_{xz} , d_{yz} orbitals and then the d_{xy} , $d_{x^2-y^2}$ orbitals are singly occupied while d_z^2 is vacant. In this situation, a Jahn–Teller distortion will occur to remove the orbital degeneracy.¹² The angle $\theta = 120^\circ$ in the TBP geometry may increase, leading toward the SP geometry at $\theta = 180^\circ$, B, or it may decrease to give a pinched TBP (PTBP) structure, C. Figure 2 shows how the orbital energies and total energy changes as the angle θ varies from 60° to 180° . Minima are observed at approximate values of $\theta = 180^\circ$ and 80° . The square pyramid is the most stable, and angles less than $70\text{--}80^\circ$ lead to unfavorable interactions between the methyl groups as they approach close to one another.

The methyl–methyl repulsions in C can be reduced by tilting the methyl groups as shown in D. As the tilt angle ϕ increases, two other effects need to be considered. First, the methyl orbital used in bonding to platinum moves off the Pt–C bond axis toward the other methyl group, and this leads to weakening of the Pt–Me bonds and the initiation of C–C bond formation, as required in the reductive elimination. Second, one C–H bond of each methyl group approaches the platinum center, as required for an agostic CH interaction. Some tilting of the methyl groups was energetically favorable. The optimum angle ϕ was dependent on the angle θ , and minimum energies were found at $\phi = 10^\circ$, $\theta = 80^\circ$; $\phi = 15^\circ$, $\theta = 70^\circ$; $\phi = 20^\circ$, $\theta = 60^\circ$. Some changes in the overlap populations with ϕ are given in Table 1. These data show that as ϕ increases, the Pt–C overlap decreases and the C–C bond overlap increases, as expected, but there is no evidence for a positive Pt \cdots H overlap. Hence, it seems that the approach of the C–H group to the platinum atom is not indicative of a positive agostic interaction but follows from the other factors discussed above. We note that after the positive effects of methyl group tilting are considered, the SP and PTBP (with θ ca. 70° and ϕ ca. 15°) structures are predicted to be very similar. Since geometry optimization is not

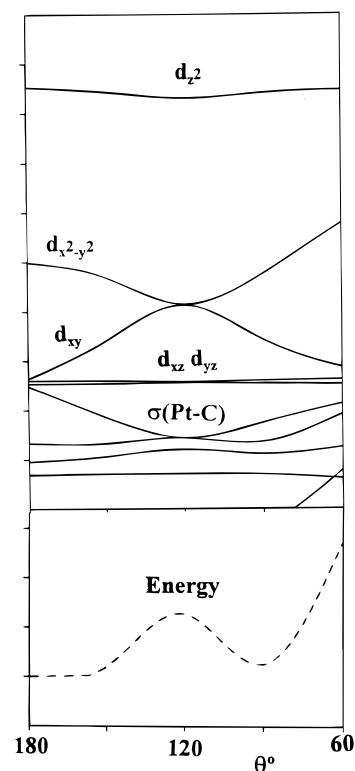


Figure 2. Dependence of individual orbital energies (above) and total energy (below) for $[\text{PtMe}_3\text{L}_2]^+$, L = PH_3 , on the angle θ defined in Chart 1.

Table 1. Mulliken Overlap Populations for $[\text{PtMe}_3(\text{PH}_3)_2]^+$, with $\theta = 60^\circ$, as a Function of the Tilt Angle ϕ

	ϕ/deg			
	0	10	20	30
OP(Pt–C) ^a	0.34	0.31	0.27	0.23
OP(C–C) ^a	0.04	0.10	0.16	0.22
OP(Pt–H) ^a	–0.02	–0.02	–0.03	–0.03
$d(\text{Pt–H})/\text{\AA}$	2.61	2.47	2.31	2.15
$\angle(\text{H–C–Pt})/\text{deg}$	109	99	89	79

^a C and H refer to the methyl carbons and the hydrogen atoms closest to platinum of the two adjacent methyl groups in structures C or D. The Pt–C distances are fixed at 2.1 Å.

usually possible using EHMO, further calculations to predict the preferred geometries of the five-coordinate complexes were carried out using density functional theory. On the basis of the EHMO calculations, it is reasonable to expect the reductive elimination to proceed directly from the PTBP structure, which could be the ground state and, if not, should at least be easily accessible from the SP structure. There is a strong correlation between the above results and those obtained for reductive elimination from T-shaped AuMe_3 by Hoffmann and co-workers.¹²

Density Functional Theory (DFT). Density functional theoretical calculations of the complexes $[\text{PtMe}_2(\text{R})\text{L}_2]^+$ were performed at the B3LYP level employing the LANL2DZ basis set, which is capable of performing calculations of third-row transition-metal complexes and is known to give close agreement between optimized and experimentally determined structures for organoplatinum complexes.¹³

The procedure was, first, to predict the ground-state structures of the platinum(IV) complex cations $[\text{PtMe}_2-$

Table 2. Calculated Energies and Charges for the Ground-State Structures

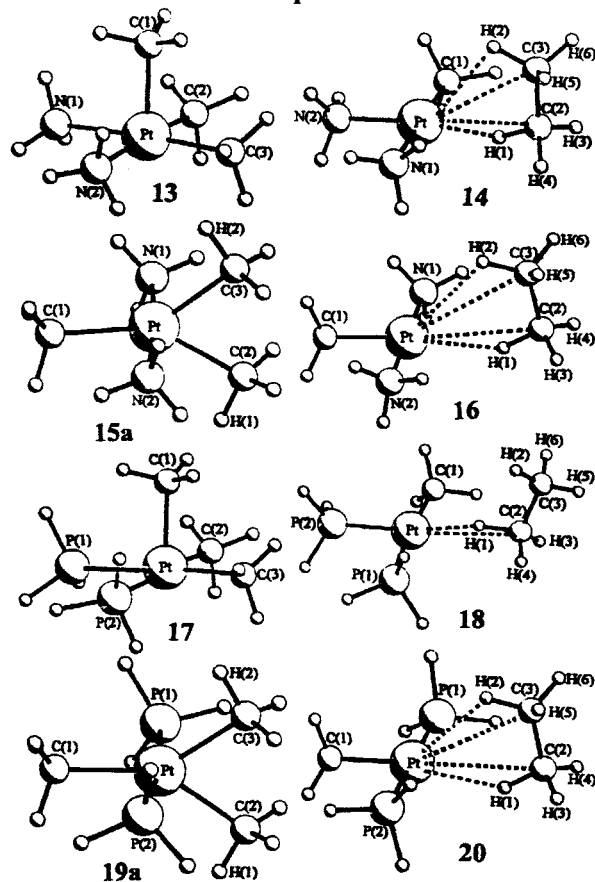
complex	total energy ^j (au)	relative energy ^h (kcal/mol)	charge ^a					
			Pt	Pt-H	Pt-Me	Pt-L ^b	Pt(CH ₄)	Pt-(C ₂ H ₆)
1	-312.49177	0	0.30	0.24	-0.02	0.25		
2	-312.49135	0	0.25	0.18	-0.04 ^e	0.25 ^c		
3	-312.50642	-9	0.43		-0.13	0.18 ^c 0.31 ^g	0.20	
6	-312.53309	-26 ⁱ	0.33		-0.05	0.29	0.16	
7	-215.89929	0	-0.02	0.24	0.02	0.37		
8	-215.89936	0	-0.07	0.20	-0.01 ^e 0.15 ^f	0.37 ^c 0.36 ^d		
9	-215.92387	-15	-0.13		-0.04	0.34 ^c 0.52 ^g	0.31	
12	-215.94021	-26 ⁱ	-0.09		0.00	0.45	0.19	
13	-351.80259	0	0.51		-0.05 ^e 0.10 ^f	0.24		
14	-351.80277	0	0.29		-0.12	0.21 ^c 0.33 ^g		0.19 [C(2)] 0.11 [C(3)]
15a	-351.77468	0	0.41		0.05 ^c -0.20 ^f	0.05		
16	-351.83325	-37	0.33		-0.04 ^g	0.28		0.06 [C(2)] 0.07 [C(3)]
17	-255.20976	0	0.16		0.00 ^e 0.14 ^f	0.34		
18	-255.22804	-11	-0.27		0.08 ^g	0.46 ^c 0.55 ^g		0.26 [C(2)] -0.08 [C(3)]
19a	-255.18460	0	-0.14		-0.09 ^g	0.52		0.09 [C(2)] 0.09 [C(3)]
20	-255.23886	-34	-0.12		0.01 ^g	0.45		0.11 [C(2)] 0.09 [C(3)]

^a The charge given for the Me, PH₃, NH₃, and CH₄ groups is for the entire ligand (including H atoms). ^b L = PH₃ or NH₃, depending on the complex. ^c Trans to Me. ^d Trans to H. ^e Trans to L. ^f Axial (no trans ligand). ^g Trans to alkane. ^h Energies of the products of Scheme 2 are reported relative to the energies of the reactants which are arbitrarily defined as zero. ⁱ The total energies of complexes **4**, **5**, **10**, and **11** could not be obtained (see text). ^j Total energy comparisons are only valid between complexes with identical ligand sets.

Structures of the Five-Coordinate Pt(IV) Complexes: SP versus PTBP Geometry. The platinum(IV) cations which give optimized square-pyramidal structures are **1**, **2**, **7**, **8**, **13**, and **17**. The greatest distortions from ideal square-pyramidal geometry were found for complexes **1** and **7**, which each have H-Pt-C angles of 83°, significantly smaller than 90°, such that the hydride ligand strongly leans toward the methyl-platinum ligands. The distortion is presumably due to electronic effects since the H-Pt-A (A = Me, L; L = NH₃, PH₃) angles in **2** and **8** are much closer to 90°; perhaps when the hydride is trans to the vacant site the partial positive charge (Table 2) leads to an attraction to the negatively charged methyl groups. In any case, the distortion leads to shorter H...C distances than in the ideal SP structure, as required for eventual methane formation.

In the complexes with SP ground states, the isomeric pairs **1** and **2**, **7** and **8** are calculated to have identical energies, so there is no preference for having the hydride or methyl group trans to the vacant site. The SP geometry with *cis*-PtL₂ groups and *fac*-PtMe₂R groups is clearly favored over the structure with *trans*-PtL₂ groups and *mer*-PtMe₂R groups (Scheme 2), and the latter structure is never the ground-state structure (see below).

The optimized structures for complexes **15a** and **19a** (eq 1, Chart 3) are very similar and possess pinched trigonal-bipyramidal geometries with mutually trans L ligands. Two of the three methylplatinum ligands (C(2) and C(3)) are positioned close to one another with a C(2)-Pt-C(3) angle of ca. 73°. This is much smaller than the expected trigonal-bipyramidal angle of 120° but surprisingly similar to the structure predicted by simple

Chart 3. PtMe₃L₂⁺ and [PtMe(C₂H₆)L₂]⁺ Complexes

EHMO calculations for **19a** (see above). The C(2)-C(3) distances of 2.56 Å are too long for the cations to be

considered as ethane complexes; the Pt–C(2) and Pt–C(3) distances range from 2.15 to 2.16 Å and, though longer than all other calculated Pt–Me distances, are still in the range of typical Pt(IV)–Me bonds.^{5,6,8} The Pt–H(1) and Pt–H(2) distances of 2.55 Å for each complex are slightly shorter than the remaining Pt–CH distances (ca. 2.78 Å) due to tilting of the methyl groups, again as predicted by the EHMO calculations. Clearly, these complexes **15a** and **19a** display structures intermediate between the square-pyramidal platinum(IV) input complexes [PtMe₃L₂]⁺ and the square-planar platinum(II) σ complex final products [PtMe(C₂H₆)L₂]⁺ and are likely to be on the path to reductive elimination of ethane from the trimethylplatinum(IV) cations. The H(1)C(2)C(3)H(2) dihedral angle of only 2.4° indicates that these C–H bonds are oriented as required to give the maximum Pt–HC interactions, and since rotation about the Pt–C bond would put these methyls in a more staggered conformation that should reduce steric interactions between the methyl groups, this may indicate that the agostic interaction is real.

What causes the change in the ground-state geometry from SP to PTBP? When two strong σ -donor ligands are mutually trans, there is a destabilizing effect (antisymbiosis), and given a choice, the platinum complexes avoid this grouping. This is why the PtMe₃ or PtMe₂H groups in platinum(IV) complexes always adopt the *fac* stereochemistry. In structures **15** and **19** (Scheme 2, eq 1), the mutually trans methyl groups destabilize the SP structure, thus the PTBP structure is more stable. Note that for isomers of [PtMe₃(PH₃)₂]⁺, **17** (SP, *cis* phosphines) is calculated to be 16 kcal mol⁻¹ more stable than **19a** (PTBP, *trans* phosphines) and the preference for **17** over **19** (Scheme 2) will then be even greater. In general, one can predict that the relative stability of the SP compared to the PTBP structure will follow the trend **13** > **17** > **15**, **19**, the same as the trans-influence series for the trans ligands, and it seems that the preferred structure switches to PTBP at the end of this series. It is expected by analogy that the cations **4**, **5**, **10**, and **11** would also prefer the PTBP structure over the SP one, but since the reductive elimination to the methane complexes **6** and **12** is so easy, this prediction could not be tested. Since the PTBP structure is probably on the route to reductive elimination, the above hypothesis is at least very reasonable.

Structures of the Alkane Complexes. The methane complexes (**3**, **6**, **9**, and **12**) all display very similar Pt–(CH₄) bonding characteristics. The methane ligand is coordinated to platinum(II) in an η^3 fashion via two C–H σ bonds with the H(1)–C(1)–H(2) plane nearly orthogonal to the PtL₂C₂ coordination plane and the A–Pt–C(1) (A = ligand trans to C(1)) angle close to 180° (Table 3). The platinum–methane Pt–HCH₃ and Pt–CH₄ distances are significantly longer than for typical hydridoplatinum(IV) and methylplatinum(IV) bond distances, respectively, suggestive of only a very weakly coordinating methane ligand.^{2a,b} There are different degrees of asymmetry in the platinum–methane unit, with the Pt–H(1) bond slightly shorter than the Pt–H(2) bond (Chart 2 and Table 3); with such long bond distances, a soft potential-energy surface is indicated.

The ethane complexes **14**, **16**, **18**, and **20** are characterized by a normal C–C single bond distance (C(2)–

Table 3. Comparison of Bond Distances and Angles and Relative Energies for the Pt(IV), Transition-State, and Pt(II) Complexes for 1, 3, 21 and 7, 9, 22^a

	1	21[#]	3	7	22[#]	9
Pt–H(1)	1.53	1.57	1.90	1.53	1.58	2.07
Pt–C(1)	2.07	2.16	2.50	2.09	2.17	2.59
Pt–C(2)	2.07	2.07	2.06	2.09	2.09	2.09
Pt–X(1) ^b	2.28	2.28	2.27	2.59	2.58	2.55
Pt–X(2) ^b	2.28	2.17	2.06	2.60	2.50	2.32
Pt–H(2)	2.59	2.50	2.43	2.59	2.50	2.38
C(1)–H(1)	2.43	1.68	1.14	2.43	1.75	1.12
H(1)–Pt–X(2)	100.3	148.3	159.6	99	141	157
H(1)–Pt–C(1)	83	50	26	83	53	25
Pt–C(1)–H(2)	105	95	46	104	94	67
relative energy	9	12	0	15	19	0

^a Distances are given in angstroms, angles in degrees, and relative energies in kcal mol⁻¹, with respect to the Pt(II)–methane complex. The symbol [#] represents a transition-state structure.^b X = N or P.

C(3) = 1.53–1.55 Å),⁸ by long Pt–C(2) and Pt–C(3) distances (ranging from 3 to 3.9 Å), and by H–C–H and C–C–H angles about C(1) and C(2) close to the tetrahedral angle; all of these features indicate a weak platinum–ethane interaction (Chart 3, Tables 4 and 5). The complexes **14**, **16**, and **20** all display a similar Pt–(C₂H₆) geometry with the ethane C(2)–C(3) vector nearly orthogonal to the PtMeL₂ coordination plane and ethane in an approximately eclipsed conformation (H(1)–C(2)C(3)H(2) dihedral angle 1.2–7.7°). This conformation allows the platinum to interact with both the C(2)–H(1) and C(3)H(2) σ bonds, but the binding is unsymmetrical, with the Pt–C(2) bond typically being shorter than the Pt–C(3) bond and with C(2) positioned close to the PtL₂Me plane and C(3) out of this plane. The long Pt–H distances (2.2–2.9 Å) and Pt–C distances (3.1–3.6 Å) within the platinum–ethane unit indicate weak binding, with the PtC(2)H(1) interaction stronger than the PtC(3)H(2) interaction. However, even the weaker interaction appears to be great enough to overcome the preference of ethane for the staggered conformation, which is about 3 kcal mol⁻¹ in free ethane. In complex **18**, the ethane is coordinated via the C(2)–H(1) σ bond only and anti to the C(1)–C(2) bond and the ethane is in the staggered conformation (H(1)C(2)–C(3)H(2) dihedral angle of 49.4°). It is not obvious why this change occurs, and the energy differences between the different forms are probably very small.

In terms of energy, the platinum(II) alkane complexes are invariably calculated to be at lower energy than the platinum(IV) precursors, although the difference is very small for **13** and **14**. For the platinum(II) alkane complexes, the *trans* isomers **6**, **12**, **16**, and **20** are all at considerably lower energy than the corresponding *cis* isomers **3**, **9**, **14**, and **18**, respectively, the difference being greater for the amine complexes compared to phosphine complexes and for ethane complexes compared to methane complexes (Tables 3–5). Since the alkane is weakly bound, it is most favorable to have it positioned *trans* to a high *trans*-influence ligand and the stability follows the series of *trans* influence Me > PH₃ > NH₃.

Transition-State Structures. Transition-state structures were investigated for the PtHMe to Pt(CH₄) transformations **1** to **3** and **7** to **9**. The resulting

Table 4. Comparison of Bond Distances and Angles and Relative Energies for the Pt(IV), Transition-State, and Pt(II) Complexes for 13, 14, 23 and 17, 18, 24, 25^a

	13	23 [#]	14	17	24 [#]	25 [#]	18
Pt–C(1)	2.07	2.07	2.06	2.09	2.07	2.10	2.08
Pt–C(2)	2.06	2.28	2.84	2.08	2.29	2.87	3.02
Pt–C(3)	2.06	2.28	3.40	2.08	2.27	3.27	3.94
Pt–X(1) ^b	2.29	2.28	2.27	2.62	2.40	2.56	2.55
Pt–X(2) ^b	2.29	2.12	2.06	2.62	2.28	2.33	2.32
Pt–H(1)	2.59	2.30	1.84	2.59	2.30	1.98	1.89
Pt–H(2)	2.60	2.27	2.95	2.60	2.27	2.94	3.94
C(2)–C(3)	2.94	1.95	1.55	2.92	1.94	1.54	1.53
C(2)–Pt–C(3)	94	51	27	88	50	28	20
X(2)–Pt–C(2)	176	154	180	174	144	179	176
X(2)–Pt–C(3)	88	155	153	89	162	152	157
Pt–C(2)–H(1)	106	77	23	104	77	31	8
Pt–C(3)–H(2)	106	75	57	105	76	63	82
H(1)C(2)C(3)H(2)	81	44	8	72	50	60	49
relative energy	0	26	0	11	36	1	0

^a Distances are given in angstroms, angles in degrees, and relative energies in kcal mol⁻¹, with respect to the Pt(II)–ethane complex. The symbol # represents a transition-state structure. ^b X = N or P.

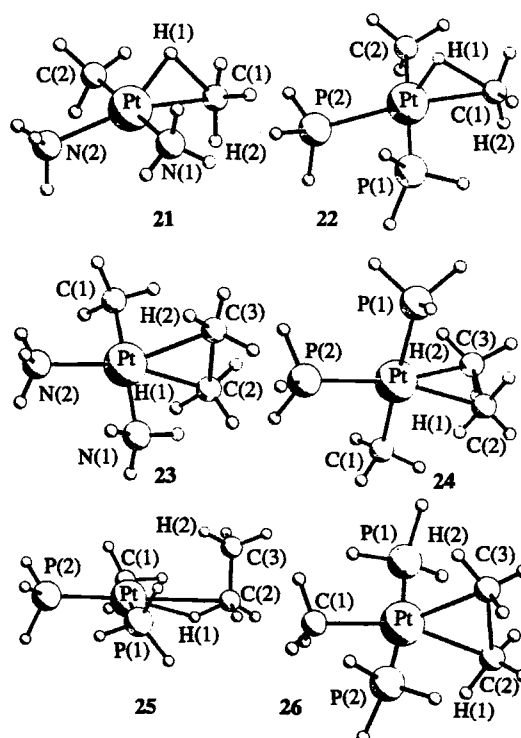
Table 5. Comparison of Bond Distances and Angles and Relative Energies for the Pt(IV) Transition-State, and Pt(II) Complexes for 19a, 20, 26^a

complex	19a	26	20
Pt–C(1)	2.17	2.11	2.07
Pt–C(2)	2.16	2.31	3.12
Pt–C(3)	2.16	2.31	3.31
Pt–P(1)	2.41	2.40	2.40
Pt–P(2)	2.41	2.40	2.40
Pt–H(1)	2.55	2.38	2.24
Pt–H(2)	2.55	2.38	2.60
C(2)–C(3)	2.56	2.10	1.55
C(2)–Pt–C(3)	73	54	30
C(1)–Pt–C(2)	143	153	180
C(1)–Pt–C(3)	144	152	152
Pt–C(2)–H(1)	97	80	42
Pt–C(3)–H(2)	97	80	31
H(1)C(2)C(3)H(2)	2	41	1
relative energy	34	41	0

^a Distances are given in angstroms, angles in degrees, relative energies in kcal mol⁻¹, with respect to the Pt(II)–ethane complex. The symbol # represents a transition-state structure.

structures are shown as **21** and **22** in Chart 4, and selected distances and energies are listed in Table 3; the structures **21** and **22** are very similar. In the transition-state structures, the hydride H(1) moves significantly toward the methyl group C(1)H₃ but there are only modest increases in the Pt–H(1) and Pt–C(1) distances (Table 3), which are much longer in the final methane complexes. Thus, these may be described as early transition states. The Pt–H(2) distance in the transition state is calculated to be 2.50 Å, which is probably too long to indicate a significant agostic interaction. In the transition state, the Pt–N(2) or Pt–P(2) distance decreases significantly. Thus, although the methyl group remains trans to N(2) or P(2) in the transition state, as the methyl group σ orbital tilts toward the hydride to begin forming the new C–H bond, the trans influence of the methyl group decreases significantly. The C(1)–H(1) distance in the transition state is calculated to be 1.68 and 1.75 Å in **21** and **22**, respectively, and once this C–H bond formation becomes significant, the energy drops quickly.

The activation energy for reductive elimination from **1** or **3** was the same at only 3 kcal mol⁻¹, but the activation energy for methane activation was calculated

Chart 4. Transition-State Structures

to be 12 and 19 kcal mol⁻¹ for **3** and **9**, respectively (Figure 3). Thus, the calculations indicate that the reductive elimination is thermodynamically more favorable for the phosphine over the amine complex but that the activation energies are essentially the same. Of course, an activation energy of only 3 kcal mol⁻¹ is indicative of a very easy reaction in both cases, consistent with experimental observations.

For ethane reductive elimination, transition-state structures were sought between **13**, **14**; **17**, **18**, and **19a**, **20**. Two transition states were found between **17** and **18**. The structures are shown as **23**–**26** in Chart 4, and data are given in Tables 4 and 5. The transition-state structures for reductive elimination of ethane from **13** and **17** are similar and are shown as **23** and **24**. The geometry can be regarded as an extreme form of the PTBP structure. Thus the C(2)–Pt–C(3) angle is about 50° in each structure, and the midpoint of the C(2)–

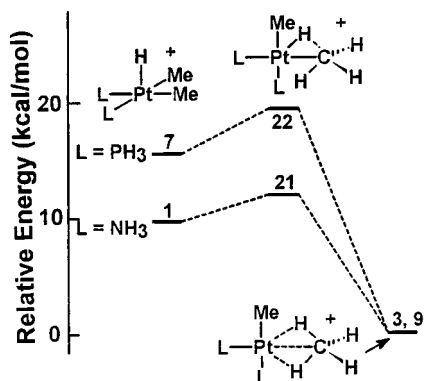


Figure 3. Relative energies of the platinum(IV) complexes $cis\text{-[PtL}_2\text{HMe}_2]^+$ and transition states $cis\text{-[PtL}_2\text{Me(HCMe)]}^+$ with respect to the platinum(II) methane complexes $cis\text{-[PtL}_2\text{Me(CH}_4\text{)]}^+$, for $L = \text{NH}_3$ or PH_3 .

C(3) bond lies trans to N(2) or P(2). Considerable tilting of the methyl groups toward each other is shown by the decrease in the angles Pt–C(2)–H(1) and Pt–C(3)–H(2) to 75–77° from the tetrahedral angles in **13** and **17**. However, the distances Pt–H(1) and Pt–H(2) of 2.27–2.30 Å and, particularly, the dihedral angles H(1)C(2)–C(3)H(2) of 44° and 50° in **23** and **24**, respectively, do not appear consistent with a significant agostic interaction, for which the dihedral angle would be expected to be close to zero to give the closest possible Pt···H contact. The staggered conformation of the two methyl groups in **23** and **24** appears to arise to minimize steric interactions between the other methyl protons. Overall, the structures are those expected if there is a three-center two-electron bond between the two carbon atoms of the methyl groups and the cationic platinum center.

The above structures correspond to a later transition state than for methane reductive elimination and the calculated activation energies are higher. In both cases, an activation energy of 25 kcal mol⁻¹ is calculated. There is an apparent discrepancy here with respect to experimental observations, since reductive elimination appears to be much easier with phosphine than with amine or imine complexes.^{5–8} A possible rationalization of this surprising result is that the reductive eliminations with phosphine complexes are accelerated by the bulky substituents that are normally present but are not considered in the model complexes.^{13d} The activation energy for C–C bond activation from **14** or **18** is calculated to be 26 and 36 kcal mol⁻¹, respectively, and should be easier with amine complexes. Of course, C–H activation would be a much easier process than C–C activation as discussed above.

The second transition state discovered between **17** and **18** corresponds to a weak ethane complex and is shown as **25**. Recall that in **18** the ethane binds through a C–H bond anti to the C–C bond. In transition state **25**, the ethane binds through a C–H bond that is syn to the C–C bond as needed for C–C bond activation. In **25**, the ethane is in the staggered conformation, and it is probable that there is another ethane complex **18a** (Figure 4) on the reaction coordinate in which the ethane is in the eclipsed conformation found in the other ethane complexes such as **14**; this complex **18a** must be slightly higher in energy than **18** so that attempts to find a ground-state geometry lead back to **18**. Note that **25** is only 1 kcal mol⁻¹ higher in energy than **18**,

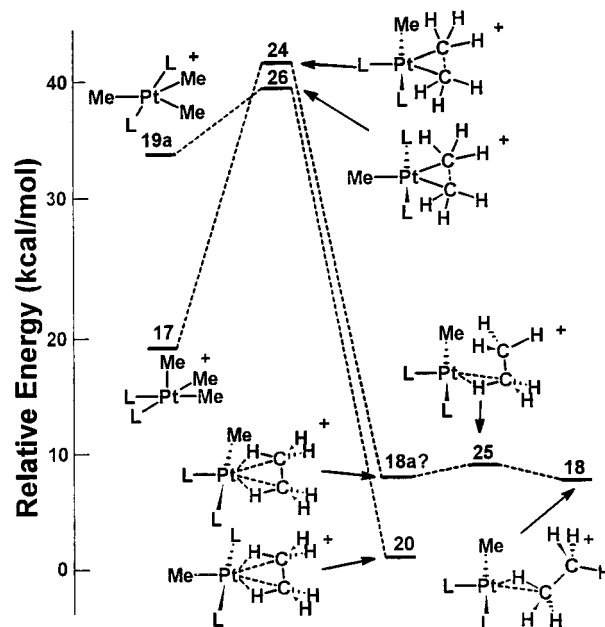


Figure 4. Relative energies of the platinum(IV) complexes $[\text{PtL}_2\text{Me}_3]^+$, transition states, and platinum(II) ethane complexes $[\text{PtL}_2\text{Me(C}_2\text{H}_6\text{)]}^+$ for $L = \text{PH}_3$ as a function of stereochemistry.

and so rearrangement of the coordinated ethane between conformers is calculated to be extremely facile.

Finally, the transition-state structure between the PTBP complex **19a** and the ethane complex **20** was calculated and is shown as **26** in Chart 4. The geometry of the platinum–ethane group is similar to those for **23** and **24**, and data are given in Table 4. The chief difference is that the Pt–C distances and C–C distance for the forming platinum–ethane group are each longer than in **23** and **24**, probably due to the strong trans influence of the trans methyl group. It is interesting that in both **19a** and **20** the methyl groups of the forming ethane unit are eclipsed, but in the transition state **26** they are closer to the staggered conformation with a dihedral angle H(1)C(2)C(3)H(2) = 41°; this probably arises due to steric effects between the other C–H protons in the transition state, and again, it suggests that agostic CH···Pt interactions are probably not very significant in the transition state. The activation energy for the reductive elimination from the PTBP structure **19a** is only 7 kcal mol⁻¹, very much less than for the SP structures **13** and **17** (Figure 4). This strongly supports the hypothesis that the PTBP structure lies on the reaction coordinate for reductive elimination even from the SP complexes, although we have not been able to detect such a complex in our calculations. Note that the activation energy for C–C bond activation from **20** is high at 41 kcal mol⁻¹.

Conclusions

The main conclusions from the DFT calculations can be summarized as follows:

1. C–H reductive elimination and oxidative addition are much easier than C–C reductive elimination and oxidative addition. For reductive elimination from SP $cis\text{-[PtL}_2\text{Me}_2\text{R]}^+$, the activation energies are 3 and 25 kcal mol⁻¹ when R = H and Me, respectively.

2. Surprisingly, the activation energies for either C–H or C–C reductive elimination are calculated to be the same for L = NH₃ or PH₃.

3. The platinum(IV) complexes are relatively more stable when L = NH₃ than when L = PH₃ compared to the platinum(II) alkane complexes. As a result, the activation energies for C–H or C–C oxidative addition are calculated to be lower for the NH₃ complexes. This is illustrated for the case of C–H reductive elimination/oxidative addition in Figure 3;¹⁴ in this case, the activation energies for C–H oxidative addition are 12 and 19 kcal mol⁻¹ for L = NH₃ or PH₃, respectively.

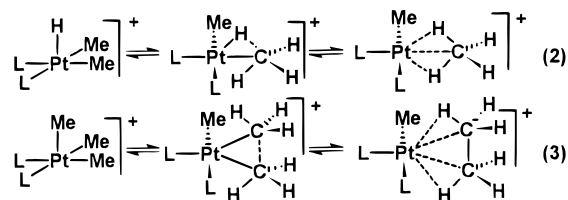
4. The platinum(IV) complexes are most stable with ligands L mutually cis in the SP stereochemistry. If the ligands L are mutually trans, the PTBP stereochemistry is preferred over the SP structure. In the platinum(II) alkane complexes, the stereochemistry with ligands L mutually trans is preferred. Since there appears to be no very low activation energy process for cis–trans isomerization, the stereochemistry of the PtL₂ group is retained in the oxidative-addition/reductive-elimination steps (Figure 4).

6. In the oxidative-addition/reductive-elimination reactions, there is probably a PTBP complex on the reaction coordinate. For C–H reductive elimination, the methane remains coordinated to platinum through the C–H σ complex. For C–C reductive elimination, the transition state is considered as a C–C σ complex, but in the final ethane complex, the binding is as a C–H σ complex (Figure 4).

7. The platinum(II)–alkane bonding is weak, and the alkane is likely to be displaced rapidly by solvent or anion in solution. It is, therefore, not surprising that these species cannot be detected directly, although there is evidence that the methane complexes may survive long enough to allow the back C–H oxidative addition to occur reversibly.^{2,5} For methane complexes, the binding is η^3 but one platinum C–H contact is shorter than the other. For ethane complexes, the binding is usually η^4 through two eclipsed platinum C–H σ -complex interactions but one appears much stronger than the other. The weaker of these σ -complex interactions is just strong enough to overcome the tendency of ethane to adopt the staggered conformation (ca. 3 kcal mol⁻¹).

(14) Frisch, M. J.; Trucks, G. W.; Schlegel, H. B.; Gill, P. M. W.; Johnson, B. G.; Robb, M. A.; Cheeseman, J. R.; Keith, T.; Petersson, G. A.; Montgomery, J. A.; Raghavachari, K.; Al-Laham, M. A.; Zakrzewski, V. G.; Ortiz, J. V.; Foresman, J. B.; Cioslowski, J.; Stefanov, B. B.; Nanayakkara, A.; Challacombe, M.; Peng, C. Y.; Ayala, P. Y.; Chen, W.; Wong, M. W.; Andres, J. L.; Replogle, E. S.; Gomperts, R.; Martin, R. L.; Fox, D. J.; Binkley, J. S.; Defrees, D. J.; Baker, J.; Stewart, J. P.; Head-Gordon, M.; Gonzalez, C.; Pople, J. A. *Gaussian 94, Revision E.1*; Gaussian, Inc.: Pittsburgh, PA, 1995.

The primary reactions for reductive elimination from the cis complexes are shown in eqs 2 and 3, of which the C–H reductive elimination is much easier than the C–C reductive elimination. It follows, from microscopic



reversibility, that C–H activation will always be much easier than C–C activation for ethane, and C–C activation can only be expected in related systems if the C–H activation is rapid and reversible while the slower C–C activation is irreversible. It may be difficult to satisfy these requirements, and so selective C–C bond activation of ethane is likely to present a major challenge.

Computational Methods

The EHMO calculations were carried out using the program CACAO with standard parameters supplied with the software and using typical bond distances found in related compounds.¹⁶ All DFT calculations were performed with the Gaussian-94 software package¹⁴ using a Cray-J90se supercomputer. Input structures were generated by MMX minimization of hand-drawn structures. All optimizations and energy calculations were performed at the B3LYP density functional theory level employing a LANL2DZ double- ζ basis set with no geometrical constraints.^{13,14} This is associated with the relativistic effective core potential for platinum and nonrelativistic effective core potential for phosphorus; validation of the use of this methodology for platinum complexes (including phosphine complexes) has been reported elsewhere.^{13a} On average, optimizations required ca. 40 h of CPU time to reach final convergence. Transition-state structures were found by using the synchronous transit-guided quasi-Newton (STQN) method, with beginning structures having bond parameters midway between reagent and product or, when this method failed, having guessed structures.¹⁴ The transition states were confirmed by vibrational analysis at the stationary point.¹⁴

Acknowledgment. We thank the NSERC (Canada) for financial support and Dr. K. I. Goldberg for helpful discussions.

OM9709291

(15) In Figure 3, the platinum(II) methane complexes are arbitrarily placed at the same energy for L = NH₃ and PH₃ to illustrate the relative energies in the two cases. In terms of absolute energies, it could be argued that a phosphine stabilizes platinum(II) or destabilizes platinum(IV) with respect to an amine ligand.

(16) Mealli, C.; Proserpio, D. M. *J. Chem. Educ.* **1990**, *67*, 399.